International Journal of Solids and Structures 48 (2011) 3462–3470

Contents lists available at SciVerse ScienceDirect

International Journal of Solids and Structures

journal homepage: www.elsevier.com/locate/ijsolstr

# Green's functions for a loaded rolling tyre

Ines Lopez Arteaga *

*Dynamics and Control Group, Department of Mechanical Engineering, Eindhoven University of Technology, 5600 MB Eindhoven, The Netherlands*
*The Marcus Wallenberg Laboratory for Sound and Vibration Research, KTH Royal Institute of Technology, 100 44 Stockholm, Sweden*

ARTICLE INFO

*Article history:*
Received 9 April 2011
Received in revised form 24 August 2011
Available online 16 September 2011

*Keywords:*
Green's function
Tyre
Rotation
Vibrations
Eigenvalues

ABSTRACT

A new formulation to determine the unit impulse response (Green's) functions of a loaded rotating tyre in the vehicle-fixed (Eulerian) reference frame for tyre/road noise predictions is presented. The proposed formulation makes use of the set of eigenfrequencies and eigenmodes for the statically loaded tyre obtained from a finite element (FE) model of the tyre. A closed-form expression for the Green's functions of a rotating tyre in the Eulerian reference system as a function of the eigenfrequencies and eigenmodes of the statically loaded tyre is found. Non-linear effects during loading are accounted for in the FE model, while the frequency shift due to the rotational velocity is included in the calculation of the Green's functions. In the literature on tyre/road noise these functions are generally used to determine the tyre response during tyre/road contact calculations. The presented formulation opens the possibility to solve the contact problem directly in the Eulerian reference frame and to include local tyre softening due to non-linear effects while keeping the computational advantage of describing the tyre dynamics as a set of impulse response functions. The advantage of obtaining the Green's functions in the Eulerian reference system is that only the Green's functions corresponding to the potential contact zone need to be determined, which significantly reduces the computational cost of solving the tyre/road contact and since the mesh is fixed in space, a finer mesh can be used for the potential contact zone, improving the accuracy of the contact force calculations. Although these effects might be less pronounced if a more accurate tyre model is used, it is found that using the Green's functions of the loaded tyre in a contact force calculation leads to smaller forces than in the unloaded case, lower frequencies are present in the response and they decrease faster as the rotational velocity increases.



## 1. Introduction

Tyre vibrations are an important source of noise inside and outside the vehicle and contribute to the energy losses through rolling resistance. Accurate and efficient models of the tyre dynamic behaviour and of the tyre/road contact interaction are needed in order to better understand how tyre vibrations contribute to the interior and exterior environment.

In the literature over tyre/road noise it is generally accepted that, due to the non-linear character of the interaction, the tyre/road contact problem must be solved in the time-domain (Fraggstedt, 2008; O'Boy and Dowling, 2009; Wullens and Kropp, 2004). However, the dynamic response of the tyre itself is often described by linear theory, linearising the equations of motion around the undeformed state and formulating the dynamic response in terms of unit impulse response functions or Green's functions (Fraggstedt, 2008; O'Boy and Dowling, 2009; Pinnington, 2006b; Rustighi et al., 2008; Wullens and Kropp, 2004, 2007). This implies that non-linear effects which occur when the tyre is loaded, due to the large deformations of the tyre belt and the hyperelastic rubber material properties, are not included.

Furthermore, these models consider a stationary (non-rotating) tyre and a contact zone which is rotating around the tyre. In other words, the contact forces and tyre dynamic response are found in the Lagrangian (tyre-fixed) reference system. In order to determine the vibration transmission to the vehicle interior or the tyre sound radiation, a description of the hub forces and the tyre vibration field in the Eulerian (vehicle-fixed) reference system is needed. This can be done by transforming the tyre response from the Lagrangian to the Eulerian frame taking into account the shift in frequencies due to the rotational velocity (Pinnington, 2006a; Sabiniarz, 2011; Wullens and Kropp, 2007). However, it has been shown that this approach does not predict the effect of rotation on a loaded tyre correctly, since the change of the tyre eigenfrequencies due to rotational velocity cannot be described with a simple shift Lopez et al. (2009).

An alternative is to use a fully non-linear FE model and apply the arbitrary Lagrangian Eulerian (ALE) formulation to obtain the dynamic tyre response in the Eulerian reference frame (Brinkmeier and Nackenhorst, 2004; Nackenhorst, 2004). In this way both the

* Address: Dynamics and Control Group, Department of Mechanical Engineering, Eindhoven University of Technology, 5600 MB Eindhoven, The Netherlands.
*E-mail addresses:* i.lopez@tue.nl, inesla@kth.se

0020-7683/$ - see front matter © 2011 Elsevier Ltd. All rights reserved.
doi:10.1016/j.ijsolstr.2011.09.006

non-linear effects due to large deformations and the influence of rotational velocity are included in the tyre response, but at a high computational cost.

Another possibility is to still model the tyre dynamic response as a collection of Green's functions but use the fully non-linear FE model to determine the static deformation due to loading and linearise the equations of motion around the deformed state (Lopez et al., 2007, 2009). In this way, the effect of the softening due to the large deformations and the non-linear material properties on the dynamic properties of the tyre is included in the linearised dynamic response, while the low computational cost of describing the tyre as a set of Green's functions is preserved.

In this paper a formulation for the Green's functions of a loaded rotating tyre in the Eulerian reference frame is proposed, based on the Modal-Arbitrary Lagrangian Eulerian (M-ALE) approach presented in Lopez et al. (2007). Particular attention is paid to the effect of load and rotational velocity on the eigenfrequencies and the implications of these effects for the Green's functions. Using this formulation to solve the tyre/road contact problem requires only a small submatrix of the total matrix of Green's functions, which reduces the size of the system matrices and, therefore, the computational cost. Furthermore, the contact forces and tyre response are directly obtained in the vehicle-fixed reference frame, which allows for a direct coupling to interior noise transmission and sound radiation.

## 2. Modal-Arbitrary Lagrangian Eulerian (M-ALE) formulation

The Modal-Arbitrary Lagrangian Eulerian (M-ALE) formulation is developed by Lopez et al. (2007) and applied to model tyre vibrations on deformed rotating tyres in the low frequency range, up to approximately 300 Hz. In the M-ALE approach the initial tyre deformation is calculated using the full FE nonlinear system of equations and, subsequently, the eigenvalues and eigenvectors of the tyre in the deformed state are calculated. These eigenvalues and eigenvectors together with the mass-matrix are extracted from the FE code and a coordinate transformation is applied to this linearised model to account for the tyre rotation. As a consequence the stiffening of the tyre due to the centrifugal forces and the Coriolis effect are included in the model. A short review of the M-ALE formulation is given here.

The dynamic equations of a tyre in an Eulerian (vehicle-fixed) reference frame can be written as

$$\ddot{\boldsymbol{\eta}}(t) + \widetilde{\mathbf{D}}(\Omega)\dot{\boldsymbol{\eta}}(t) + \widetilde{\mathbf{K}}(\Omega)\boldsymbol{\eta}(t) = \boldsymbol{\Phi}^T\mathbf{f}(t), \tag{1}$$

where the vector $\mathbf{f}(t)$ contains the applied forces in the Eulerian reference frame, $\Omega$ is the rotating velocity of the tyre, $\boldsymbol{\eta}(t)$ are the modal coordinates of the statically loaded tyre and $\boldsymbol{\Phi}$ represents the matrix of eigenvectors, such that the displacement vector in cartesian coordinates in the Eulerian reference frame is given by

$$\mathbf{x} = \boldsymbol{\Phi}\boldsymbol{\eta}. \tag{2}$$

The modified damping and stiffness matrices $\widetilde{\mathbf{D}}$ and $\widetilde{\mathbf{K}}$ are defined as

$$\widetilde{\mathbf{D}} = 2\mathbf{P}(\Omega, \mathbf{M}, \boldsymbol{\Phi}) + \mathbf{D}_{\text{mod}} \tag{3}$$

and

$$\widetilde{\mathbf{K}} = \mathbf{S}(\Omega, \mathbf{M}, \boldsymbol{\Phi}) + \mathbf{D}_{\text{mod}}\mathbf{P}(\Omega, \mathbf{M}, \boldsymbol{\Phi}) + \mathbf{K}_{\text{mod}}. \tag{4}$$

The matrices $\mathbf{P}$ and $\mathbf{S}$ are added stiffness and damping terms due to the rotation are given by

$$\mathbf{P}(\Omega, \mathbf{M}, \boldsymbol{\Phi}) = \boldsymbol{\Phi}^T\mathbf{M}\left(\widehat{\boldsymbol{\Omega}}\boldsymbol{\Phi} + \Omega\frac{\Delta\boldsymbol{\Phi}}{\Delta\theta}\right) \tag{5}$$

and

$$\mathbf{S}(\Omega, \mathbf{M}, \boldsymbol{\Phi}) = \boldsymbol{\Phi}^T\mathbf{M}\left(\widehat{\boldsymbol{\Omega}}^2\boldsymbol{\Phi} + 2\Omega\widehat{\boldsymbol{\Omega}}\frac{\Delta\boldsymbol{\Phi}}{\Delta\theta} + \Omega^2\frac{\Delta^2\boldsymbol{\Phi}}{\Delta\theta^2}\right), \tag{6}$$

where $\widehat{\boldsymbol{\Omega}}$ is the matrix relating the time derivative of the rotation matrix to the rotation matrix Lopez et al. (2007) and $\theta$ represents the spatial angular position in the vehicle-fixed reference frame.

The mass matrix, $\mathbf{M}$, is extracted from the finite element discretization and the stiffness matrix $\mathbf{K}_{\text{mod}}$ is a diagonal matrix with elements $k_{ii} = \omega_i^2$, where $\omega_i$ are the eigenfrequencies of the deformed non-rotating tyre and $i = 1,\ldots,N$ with $N$ the number of retained modes. The reduced damping matrix $\mathbf{D}_{\text{mod}}$ is the projection of the system damping matrix on the retained modes. In general $\mathbf{D}_{\text{mod}}$ can be a full matrix, since there is no fundamental assumption in the formulation that requires this matrix to be diagonal. However, as a first approximation, Rayleigh damping is assumed

$$\mathbf{D}_{\text{mod}} = \alpha\mathbf{M} + \beta\mathbf{K}, \tag{7}$$

in which $\mathbf{K}$ represents the stiffness matrix and $\alpha$ and $\beta$ are constant coefficients.

The data needed to build the matrices $\widetilde{\mathbf{D}}$ and $\widetilde{\mathbf{K}}$ are the eigenvalues and eigenvectors of the statically loaded tyre obtained from a FE analysis and the mass matrix $\mathbf{M}$ from the FE model. It should be noted that $\widetilde{\mathbf{D}}$ and $\widetilde{\mathbf{K}}$ are non-diagonal and non-symmetric matrices, which means that Eq. (1) is a coupled system of equations. Therefore the set of coordinates $\boldsymbol{\eta}(t)$ is not a set of modal coordinates of the rotating tyre in the vehicle-fixed reference frame. The approach from Lopez et al. (2007) summarized above is illustrated in Fig. 1.

Assuming a stationary harmonic excitation

$$\mathbf{f}(t) = \hat{\mathbf{f}}(\omega)e^{i\omega t} \tag{8}$$

and

$$\boldsymbol{\eta}(t) = \hat{\boldsymbol{\eta}}(\omega)e^{i\omega t}, \tag{9}$$

where $\hat{}$ denotes complex amplitude, Eq. (1) can be transformed to the frequency domain, leading to the following set of equations:

$$\hat{\boldsymbol{\eta}}(\omega, \Omega) = [-\omega^2\mathbf{I} + i\omega\widetilde{\mathbf{D}}(\Omega) + \widetilde{\mathbf{K}}(\Omega)]^{-1}\boldsymbol{\Phi}^T\hat{\mathbf{f}}(\omega). \tag{10}$$

Considering that the response in the frequency domain can be obtained as the product of a receptance matrix and the forces

$$\hat{\mathbf{u}}(\omega) = \mathbf{H}(\omega)\hat{\mathbf{f}}(\omega), \tag{11}$$

and taking the relationship in Eq. (2) into account, an expression for the receptance of the rotating tyre in the Eulerian reference frame can be derived,

$$\mathbf{H}(\omega, \Omega) = \boldsymbol{\Phi}[-\omega^2\mathbf{I} + i\omega\widetilde{\mathbf{D}}(\Omega) + \widetilde{\mathbf{K}}(\Omega)]^{-1}\boldsymbol{\Phi}^T. \tag{12}$$

The above expression gives the response at a given position and direction on the tyre to an excitation at a given position and direction on the tyre in the Eulerian reference frame and it shows that the response of the tyre depends on the rotational velocity $\Omega$ of the tyre. In practice, only the submatrix relating the forces at the

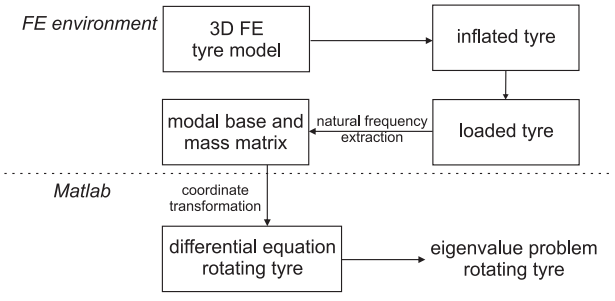


**Fig. 1.** Illustration of the approach to model vibrations on deformed rotating tyres.

contact area to the response at any position on the tyre is needed to determine the tyre response once the contact forces are known. This significantly reduces the computational effort.

## 3. Green's functions of the rotating tyre

### 3.1. Tyre/road contact interaction

It is generally accepted that the tyre/road contact problem must be solved in the time-domain due to the non-linear character of the interaction (Fraggstedt, 2008; O'Boy and Dowling, 2009; Wullens and Kropp, 2004). The usual assumption is that the dynamic behaviour of the tyre itself can be described, using linear theory, as a collection of unit impulse response functions or Green's functions. The tyre response is then calculated in the time-domain from the convolution integral between the Green's functions and the forces

$$u_j(t) = \sum_l g_{jl}(t) * f_l(t). \tag{13}$$

In Eq. (13) $u_j(t)$ is the displacement at location and direction $j$ on the tyre, $f_l(t)$ is the force at location and direction $l$ on the tyre and $g_{jl}(t)$ is the corresponding Green's function.

One way to obtain the Green's functions of the rotating tyre in the Eulerian reference frame is to calculate the receptance matrix given in Eq. (12) numerically and perform an inverse FFT transformation of this matrix. Although this is a valid approach, it has the disadvantage that the full time-history of the Green's functions has to be calculated and stored, which becomes prohibitive in terms of computer effort if long simulation times at medium frequencies are to be achieved. A computationally efficient alternative is to derive an analytical expression of the Green's functions of the rotating tyre in the Eulerian reference frame. Such an expression allows for the calculation of the Green's functions for a given time instant *on-line* during the computation of the contact forces, which dramatically reduces the storage needs and speeds up the calculations.

### 3.2. Derivation of the Green's functions

The Green's functions $g_{jl}$ of the tyre expressed in the vehicle-fixed reference frame can be determined by solving

$$\ddot{\boldsymbol{\eta}}(t) + \widetilde{\mathbf{D}}(\Omega)\dot{\boldsymbol{\eta}}(t) + \widetilde{\mathbf{K}}(\Omega)\boldsymbol{\eta}(t) = \boldsymbol{\Phi}_l^T \delta(t), \tag{14}$$

where $\boldsymbol{\Phi}_l$ is the $l$th row of $\boldsymbol{\Phi}$ and $\delta(t)$ represents the Dirac delta function. In order to find an analytical expression for the Green's function, the first step is to transform Eq. (14) to a set of first order differential equations. To this end a new vector $\mathbf{y}$ is defined as

$$\mathbf{y}(t) = \begin{bmatrix} \boldsymbol{\eta}(t) \\ \dot{\boldsymbol{\eta}}(t) \end{bmatrix} \tag{15}$$

and the first order system becomes

$$\mathbf{A}(\Omega)\dot{\mathbf{y}}(t) + \mathbf{B}(\Omega)\mathbf{y}(t) = \overline{\boldsymbol{\Phi}}_l^T \delta(t), \tag{16}$$

with

$$\mathbf{A}(\Omega) = \begin{bmatrix} \widetilde{\mathbf{D}}(\Omega) & \mathbf{I} \\ \mathbf{I} & \mathbf{0} \end{bmatrix}, \quad \mathbf{B}(\Omega) = \begin{bmatrix} \widetilde{\mathbf{K}}(\Omega) & \mathbf{0} \\ \mathbf{0} & -\mathbf{I} \end{bmatrix} \quad \text{and} \quad \overline{\boldsymbol{\Phi}}_l^T = \begin{bmatrix} \boldsymbol{\Phi}_l^T \\ \mathbf{0} \end{bmatrix}. \tag{17}$$

The system of Eq. (16) is a set of coupled differential equations. Because $\mathbf{A}$ and $\mathbf{B}$ are non-symmetric matrices, the general algebraic eigenvalue problem and the adjoint eigenvalue problem have to be solved in order to transform Eq. (16) into a set of uncoupled first order differential equations. The general eigenvalue problem is given by

$$[s\mathbf{A} + \mathbf{B}]\mathbf{v} = 0 \tag{18}$$

and the adjoint eigenvalue problem can be written as

$$[s\mathbf{A} + \mathbf{B}]^T\mathbf{w} = 0, \tag{19}$$

where $\mathbf{v}$ and $\mathbf{w}$ are the right and left eigenvectors respectively and the eigenvalue $s$ is the same for both eigenvalue problems. All variables in Eqs. (18) and (19) are functions of $\Omega$, but the explicit dependence is omitted for clarity. If a new variable transformation is introduced in Eq. (16)

$$\mathbf{y}(t) = \mathbf{V}\boldsymbol{\gamma}(t), \tag{20}$$

with $\mathbf{V}$ the matrix with right eigenvectors and $\gamma(t)$ the modal coordinates of the rotating tyre in the Eulerian reference frame, and premultiplying with the matrix of left eigenvectors $\mathbf{W}$ the following set of uncoupled differential equations is obtained

$$a_r[\dot{\gamma}_r(t) - s_r\gamma_r(t)] = \mathbf{w}_r^T\overline{\boldsymbol{\Phi}}_l^T\delta(t), \quad r = 1,\ldots,2N, \tag{21}$$

where

$$\mathbf{W}^T\mathbf{A}\mathbf{V} = \lceil a_r \rfloor \quad \text{and} \quad \mathbf{W}^T\mathbf{B}\mathbf{V} = \lceil -s_r a_r \rfloor \quad r = 1,\ldots,2N, \tag{22}$$

with $\lceil\ \rfloor$ indicating a diagonal matrix and $N$ the number of eigenvectors extracted from the FE analysis of the statically loaded tyre. It should be stressed that the left $\mathbf{w}_r$ and right $\mathbf{v}_r$ eigenvectors and the corresponding eigenvalues $s_r$ depend on the rotational velocity of the tyre $\Omega$.

Now it can be easily shown that the solution to Eq. (21) has the following form:

$$\gamma_r(t) = \frac{\mathbf{w}_r^T\overline{\boldsymbol{\Phi}}_l^T}{a_r}e^{s_r t}, \quad r = 1,\ldots,2N. \tag{23}$$

By combining Eqs. (2) and (20) a relationship can be found between the response at a given point of the rotating tyre in the Eulerian reference frame and the modal coordinates of the rotating tyre,

$$\mathbf{x}(t) = \overline{\boldsymbol{\Phi}}\mathbf{V}\gamma(t) \quad \text{with} \quad \overline{\boldsymbol{\Phi}} = [\boldsymbol{\Phi}\ \mathbf{0}]. \tag{24}$$

If Eq. (23) is substituted in Eq. (24) an expression for the Green's function between the excitation at a given location and direction $l$ and the response at another location and direction $j$ expressed in the Eulerian reference frame can be obtained,

$$g_{jl}(\Omega, t) = \sum_{k=1}^{N}\Phi_{jk}\left[\sum_{r=1}^{2N} v_{kr}\frac{\sum_{p=1}^{N} w_{pr}\Phi_{lp}}{a_r}e^{s_r t}\right]. \tag{25}$$

In Eq. (25) the $\Omega$ dependence of $g_{jl}$ has been explicitly included to stress the fact that the Green's functions determined by Eq. (25) are expressed in the Eulerian reference frame and that they will change if the rotational velocity changes. In practice the Green's functions are evaluated at discrete time intervals, which leads to a slightly modified form of Eq. (25)

$$g_{jl}(\Omega, m\Delta t) = \sum_{k=1}^{N}\Phi_{jk}\left[\sum_{r=1}^{2N} v_{kr}\frac{\sum_{p=1}^{N} w_{pr}\Phi_{lp}}{a_r}e^{s_r m\Delta t}\right], \quad m = 1,\ldots,M, \tag{26}$$

where $\Delta t$ is the time step used in the calculations and $T = M\Delta t$ is the total calculation time considered.

Introducing the following diagonal matrix

$$\boldsymbol{\Gamma}(\Omega, m\Delta t) = \left\lceil \frac{e^{s_r m\Delta t}}{a_r} \right\rfloor, \quad r = 1,\ldots,2N \tag{27}$$

a compact expression for the matrix of Green's functions for a rotating tyre in the Eulerian reference frame can be obtained,

$$\mathbf{G}(\Omega, m\Delta t) = \overline{\boldsymbol{\Phi}}\mathbf{V}(\Omega)\boldsymbol{\Gamma}(\Omega, m\Delta t)\mathbf{W}^T(\Omega)\overline{\boldsymbol{\Phi}}^T. \tag{28}$$

It should be noted that only the submatrix corresponding to the contact region needs to be evaluated to solve the tyre/road interaction problem, which significantly reduces the actual size of the

matrices in Eq. (27). It is also important to note that the only information needed to apply Eq. (25) are the eigenvalues and eigenvectors of the statically loaded tyre and the mass matrix $M$, which can be readily obtained from a FE model of the tyre.

## 4. Tyre model

In this section the tyre model used in the simulations is described and the influence of loading and travelling velocity on the eigenfrequencies of the tyre is shortly discussed.

### 4.1. Description of finite element (FE) tyre model

A FE model of a 185/70 SR14 tyre without tread pattern is used in this research SIMULIA (2006). The tread and sidewall consist of rubber, while the belts and carcass consist of fibre-reinforced rubber composites. The rubber is modelled as incompressible and hyperelastic. The hyperelastic behaviour of the rubber is described by a strain energy potential of the Neo-Hookean form. In addition, the fibre-reinforcements are modelled as a linear elastic material. In the circumferential direction, 72 general three-dimensional 6- and 8-node linear hybrid brick elements are used to discretise the model, each node having three active translational degrees of freedom. In total, this leads to a tyre model consisting of 6048 elements and to approximately 25,000 degrees of freedom. The tyre model is inflated to an uniform inflation pressure of 200 kPa. More detailed information about the build-up and materials of the FE model can be found in SIMULIA (2006).

This FE tyre model has been qualitatively validated for the frequency range 0–250 Hz by comparing eigenfrequencies to experimental data of tyres of similar size, as shown in Fig. 2. Here the calculated eigenfrequencies of the first symmetric mode family $(n,0)$ (with $n$ the number of wavelengths in the circumference) are compared to experimental data. However, the inner structure of the measured tyres is unknown, which prevents a direct comparison of the calculated eigenfrequencies with the measured results.

Guyan reduction is applied in order to reduce the size of the system matrices. Guyan reduction neglects inertia effects and is exact at zero frequency only, Guyan (1965). However, if the retained DOF's are selected following the guidelines reported in Bouhaddi and Fillod (1992), a reduced eigenvalue problem can be obtained which gives a maximum error < 7% between the full and reduced models in the frequency range 0–500 Hz.

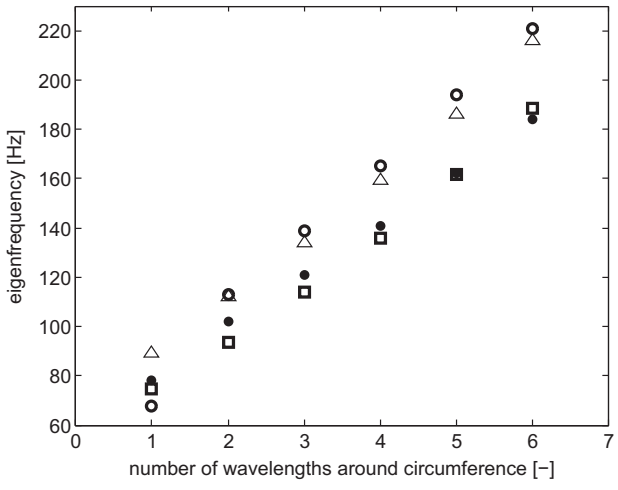


**Fig. 2.** Comparison of calculated and measured eigenfrequencies. • 185/70 R14 (calculated), △ 175/70 R13 Gong (1993), ○ 185/70 R14 Fioole (2008), □ 195/70 R14 Kim et al. (2007).

### 4.2. Influence of load on the tyre eigenfrequencies

The tyre is statically loaded onto an idealised rigid, flat and smooth surface. The normal to the surface is aligned with a radial direction in the tyre. The contact between the tyre and the smooth surface is modelled as a frictionless rigid contact. Subsequently, the tyre rim is loaded with a force in the negative vertical direction (perpendicular to the flat rigid surface) and the contact force distribution is determined. After this the rim is fixed, the contact constraint on the contact nodes is removed and the contact forces are applied on the contact nodes.

In Fig. 3 the lowest 50 calculated eigenfrequencies ordered from lowest to highest are shown for the unloaded and loaded tyre for two load values, 2750 and 4350 N. These results are in good qualitative agreement with the effect of tyre loading measured in (Kindt, 2008; Pieters, 2007). It can be seen that increasing the load from 2750 to 4350 N has a very small influence on the eigenfrequency. In the following sections only the results for the load of 2750 N will be shown, since the results for 4350 N are very similar.

### 4.3. Influence of travelling velocity on the tyre eigenfrequencies

There are three effects that make the eigenfrequencies of a rotating tyre depend on the rotational velocity and, therefore, differ from the eigenfrequencies of the non-rotating tyre. The stiffening due to the rotation leads to slightly higher eigenfrequencies and the Coriolis acceleration leads to the so-called 'bifurcation' effect, where the speed of waves propagating in opposite circumferential directions with the same wavelength are different even when observed in the Lagrangian reference system Kim and Bolton (2003). However, it has been shown that the change in eigenfrequencies due to rotational stiffening and Coriolis acceleration is negligible at the rotational velocities corresponding to the usual driving velocities Kim and Bolton (2003).

The third effect is the well-known Doppler-shift, which appears when the tyre is observed from an Eulerian (vehicle-fixed) reference system. In the case of the unloaded tyre, the two identical eigenfrequencies observed in the Lagrangian reference system split into two frequencies, one higher and one lower that the original frequency according to the relationship

$$f = f_s \pm \frac{n}{2\pi}\Omega, \tag{29}$$

where $f$ is the rotation compensated tyre eigenfrequency, $f_s$ the eigenfrequency of the non-rotating tyre and $n$ the number of wave-

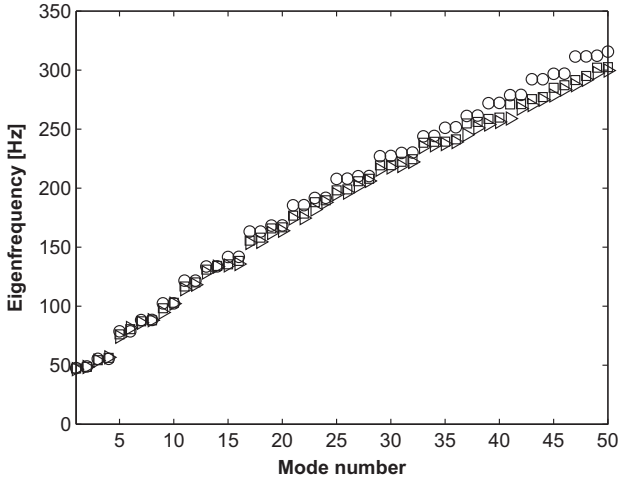


**Fig. 3.** Influence of load on eigenfrequencies. ○ unloaded tyre, □ load 2750 N, ▷ load 4350 N.

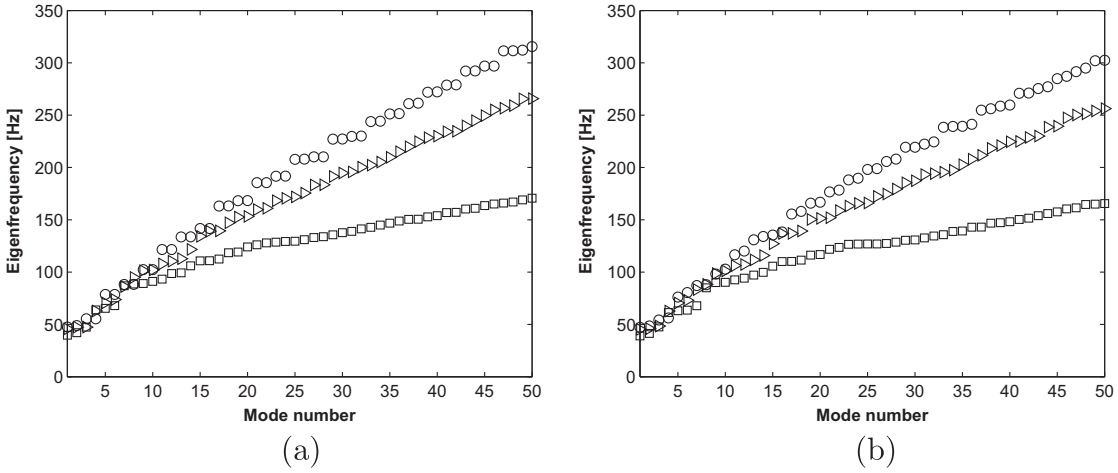


**Fig. 4.** Influence of travelling velocity on eigenfrequencies. With (a) unloaded tyre, (b) load 2750 N and ∘ 0 km/h, ▷ 60 km/h, □ 100 km/h.

lengths along the circumference Kim and Bolton (2003). According to Eq. (29) the eigenfrequencies of an unloaded rotating tyre linearly increase or decrease as the rotational velocity increases. This gives straight lines of varying slopes when the eigenfrequencies are plotted as a function of the rotational velocity. However, as shown in Lopez et al. (2009), Eq. (29) no longer holds for loaded tyres. In this case a phenomenon known as frequency loci veering occurs and the eigenfrequency lines corresponding to two modes 'bend' instead of crossing when they approach each other. This effect becomes more pronounced as the tyre load increases. Nevertheless, if the eigenfrequencies are plotted as a function of the mode number, both the unloaded and loaded tyre show the same qualitative behaviour. This is shown in Fig. 4, where the eigenfrequencies of the unloaded and loaded (load 2750 N) tyre as a function of the mode number are shown for the non-rotating tyre and two travelling velocities: 60 km/h ($\Omega$ = 55.7 rad/s) and 100 km/h ($\Omega$ = 87.8 rad/s). Note that for every value of the travelling velocity the modes are ordered from lowest to highest eigenfrequency. Both plots show a similar increase of modal density as the travelling velocity increases for both the unloaded and the loaded tyre. Therefore the net effect of increasing the travelling velocity is a decrease in the values of the eigenfrequencies and an increase of the number of modes in a given frequency range which is also reported in Brinkmeier and Nackenhorst (2008).

## 5. Calculation of the Green's functions of the rotating tyre

The tyre model described in Section 4.1 has been used to calculate the Green's functions of the loaded rotating tyre given by Eq. (28). A finer mesh is used for the potential contact zone, with a discretization of 0.8° in the potential contact zone and 4° elsewhere. The spatial gradients of the eigenvectors in Eqs. (5) and (6) are calculated by a 7 point finite difference scheme. Six hundred modes are considered in the calculations and the Rayleigh damping parameters are set to $\alpha = 30\ s^{-1}$ and $\beta = 10^{-4}$ s. These values are chosen such that the corresponding modal damping ratios are of the same order found in experiments for the frequency range 0–300 Hz (Kindt, 2008; Pieters, 2007). Furthermore all results shown below correspond to a load of 2750 N and only excitations and responses in the vertical direction (perpendicular to the road surface) are considered.

In Fig. 5(a) and (b) a schematic front view and a close-up view of the tyre at the potential contact zone can be seen where the nodes considered in the calculations are shown and numbered 1–4. Node

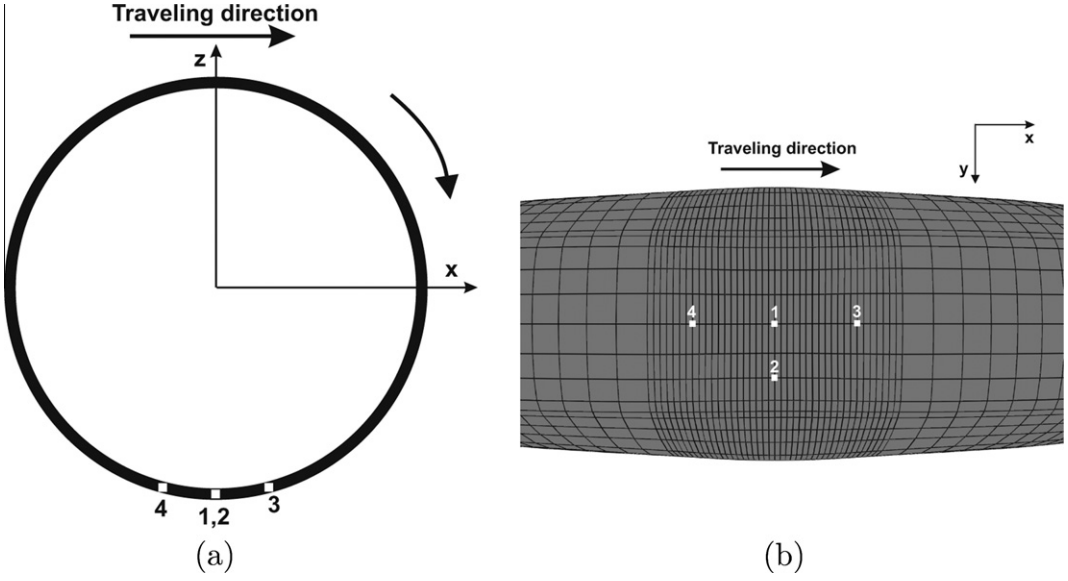


**Fig. 5.** Coordinate system and selected excitation and response locations. (a) Schematic front view of the tyre and (b) close view of the contact area.

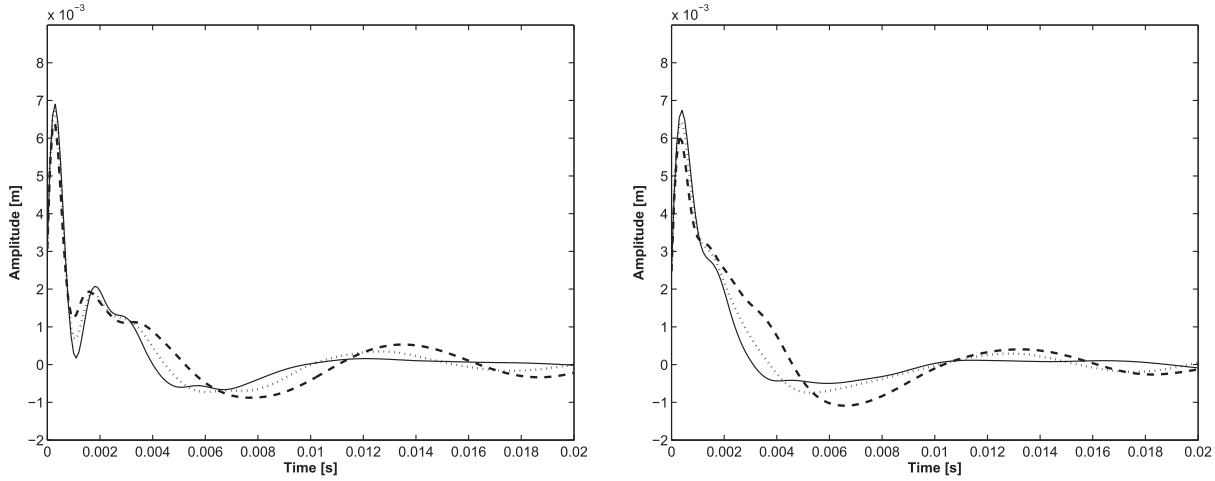


(a) $g_{11}(t,\Omega)$ (b) $g_{22}(t,\Omega)$

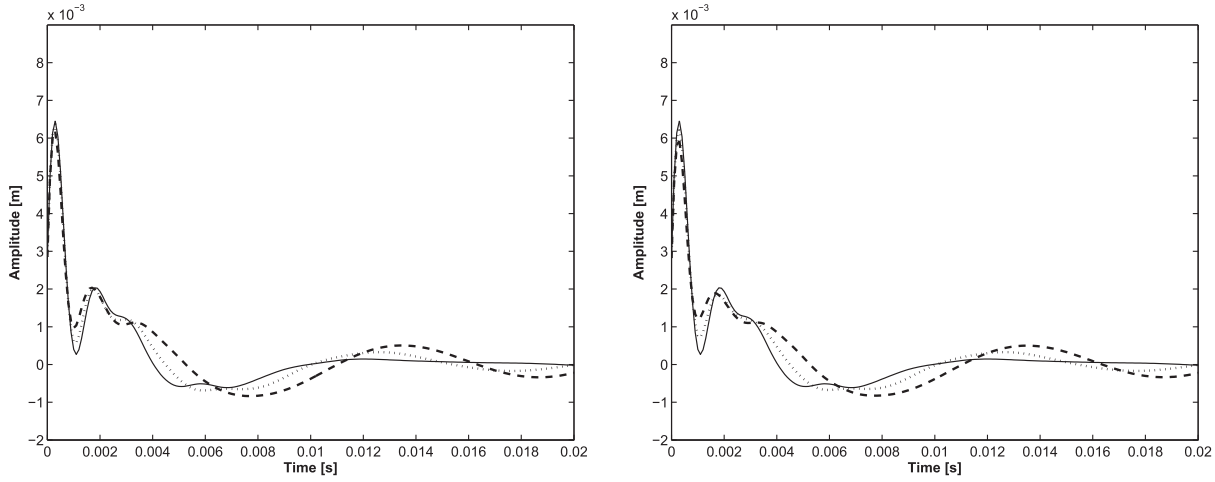


(c) $g_{33}(t,\Omega)$ (d) $g_{44}(t,\Omega)$

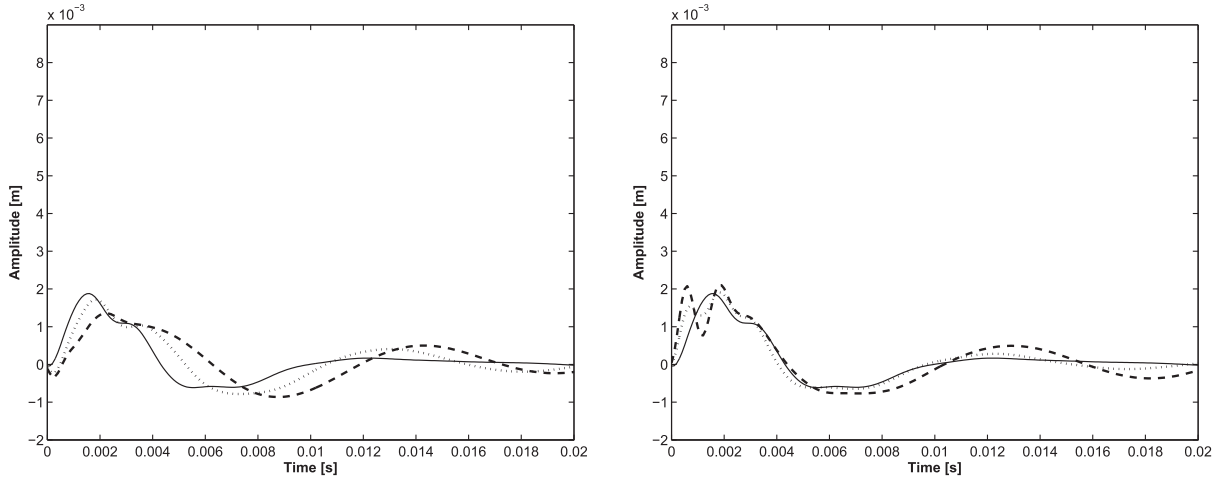


(e) $g_{31}(t,\Omega)$ (f) $g_{41}(t,\Omega)$

**Fig. 6.** Green's functions of the unloaded rotating tyre. (—) 0 km/h, (. . .) 60 km/h, (- - -) 100 km/h.

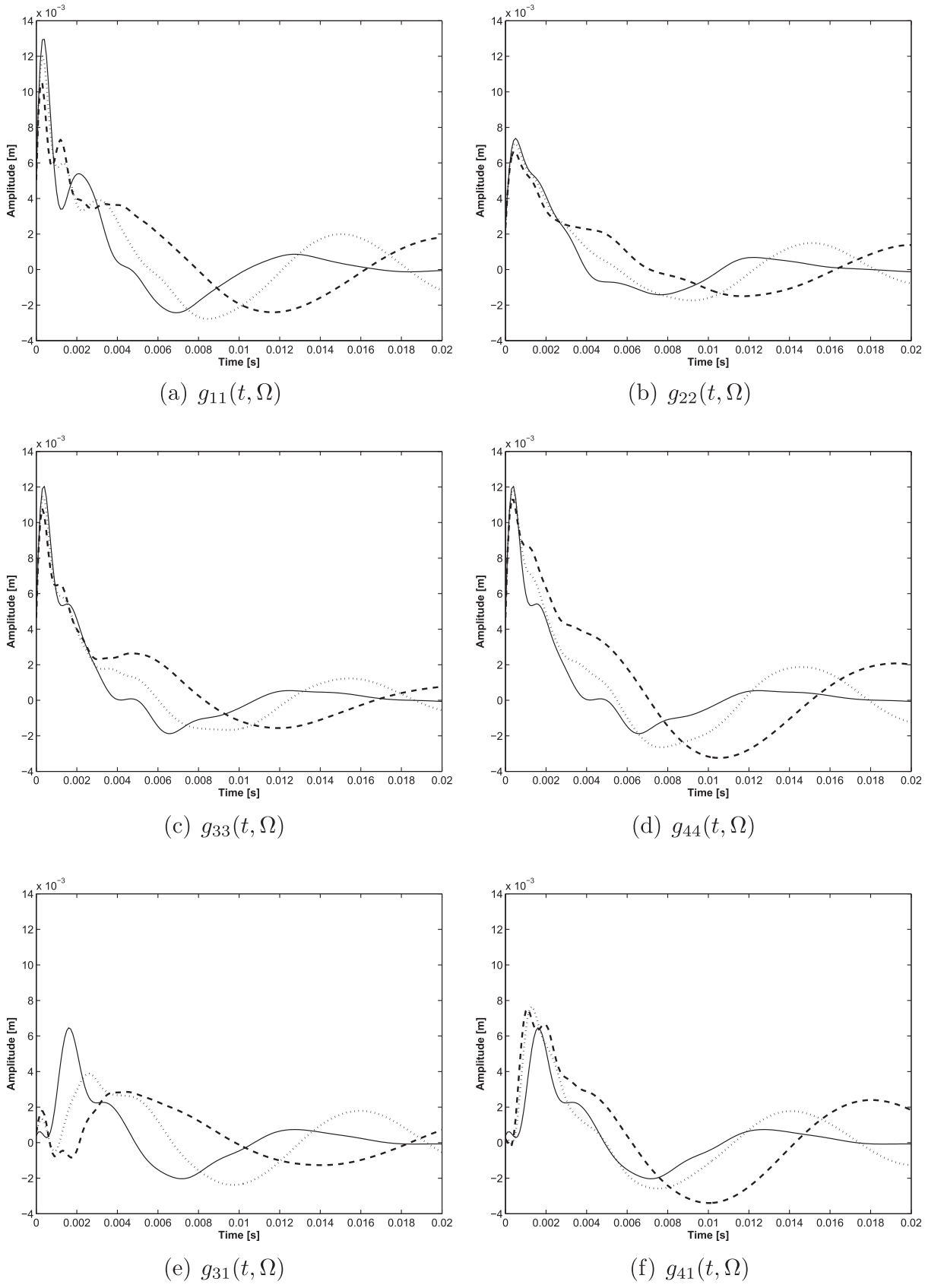


**Fig. 7.** Green's functions of the loaded rotating tyre. Load 2750 N. (—) 0 km/h, (. . .) 60 km/h, (- - -) 100 km/h.

1 is exactly in the middle of the contact area on the *yz*-plane and nodes 3 and 4 are placed symmetrically with respect to this plane, at the leading $(-10, 4^\circ)$ and trailing $(10, 4^\circ)$ edge, respectively. The angular values indicate the position of nodes 3 and 4 in the circumferential direction when the tyre is unloaded, taking the rotating direction as positive and node 1 as position 0°. These nodes are chosen to illustrate the influence of rotation on the tyre response. Node 2 is placed on the *yz*-plane at an axial distance of 0.038 m from node 1 and is chosen to show the difference in softening effect due to the loading.

The Green's functions for the unloaded and loaded tyre have been calculated with a time discretization $\Delta t = 10^{-4}$ s. Using Eq. (28) the submatrix corresponding to the four positions depicted in Fig. 5 can be determined. The results are plotted in Figs. 6 and 7 for the unloaded and loaded tyre respectively. The Green's functions are shown in the time interval [0–0.02] s and the same vertical axis scaling is used for all plots in Fig. 6 and for all plots in Fig. 7, but a different vertical axis scaling is used in each of these figures. Results for three velocities are presented: 0 km/h (solid line), 60 km/h (dotted line) and 100 km/h (dashed line).

The point-Green's functions of the unloaded tyre in Fig. 6(a–d) show all a qualitatively similar pattern, with an initial response peak which is only slightly affected by the travelling velocity, both in height and width. This is possibly due to the fact that the highest eigenfrequency included in the model is approximately 800 Hz, with a corresponding time period of about 1.2 ms. The influence of the travelling velocity becomes apparent after the first millisecond, where the period of the response increases with increasing travelling velocity.

The functions $g_{33}$ and $g_{44}$ in Fig. 6(c) and (d) are particularly interesting. For a non-rotating tyre (solid line) both Green's functions are identical, since points 3 and 4 are located symmetrically with respect to the *yz*-plane and the vertical excitation is symmetrically applied as well. As the travelling velocity increases, small differences in the response during the first 2 ms (frequencies above 500 Hz) can be seen, but the responses are practically identical for subsequent time steps. The rotation of the tyre disturbs the symmetry of the system with respect to the *yz*-plane while the excitation is still symmetric with respect to this plane. The radial component of the excitation is the same at nodes 3 and 4, but the tangential component points against the rotation at node 3 and in the direction of rotation at node 4. Since the tangential component is small for an angle of $10, 4^\circ$, the difference between $g_{33}$ and $g_{44}$ is small as well.

The cross-Green's functions $g_{31}$ and $g_{41}$ shown in Fig. 6(e) and (f) give the vertical response at node 3 and 4, respectively for a vertical excitation at node 1. As one would expect, these two responses are identical for the non-rotating tyre. As the travelling velocity increases differences between these two Green's functions become apparent. From node 1 to node 3 at the leading edge, waves have to travel against the rotation, which increases the time for the perturbation to reach node 3. On the other hand, from node 1 to node 4 at the trailing edge waves travel with the rotation, which decreases the time for the perturbation to reach node 4.

In the case of the loaded rotating tyre, larger differences between the Green's functions are found, as shown in Fig. 7. The initial response peak in the point-Green's functions and the amplitude of the subsequent response is larger than in the case of the unloaded tyre, particularly for the nodes located on the centre line of the contact area in the longitudinal direction. This is due to the softening occurring at the contact patch when the tyre is loaded, which is specially pronounced in the middle of the contact area. Although this effect is overestimated in the current FE model, due to the relatively simple model of the belt structure, the response at node 2 is in reasonable agreement with experimental data O'Boy and Dowling (2009). A better estimation of the softening at the contact patch will be obtained if a more realistic model of the belt structure is used. It should be noted that this decrease in stiffness at the contact patch can only be predicted if the large deformations due to loading are determined using a non-linear model. It can also be seen that the period of oscillation increases as the rotational velocity increases and this effect is again more pronounced than for the unloaded tyre.

Unlike in the case of the unloaded tyre, the point-Green's functions $g_{33}$ and $g_{44}$ for the loaded tyre in Fig. 7(c) and (d) are no longer similar when the tyre is rotating and the difference becomes more pronounced as the travelling velocity increases. For a travelling velocity of 100 km/h the response at the leading edge has a lower amplitude and larger period than the response at the trailing edge. This behaviour can be explained by looking at the eigenmodes of the loaded rotating tyre, which are not axi-symmetric, due to the loading, and are not symmetric with respect to the vertical plane perpendicular to the travelling direction, due to the rotational velocity and the effect of frequency-loci veering Lopez et al. (2009). Since the leading edge is stiffer than the trailing edge, these Green's functions will lead to a non uniform force distribution, with the resultant vertical force acting at the front of the contact patch and moving away from the centre of the contact patch as the travelling velocity increases.

Regarding the cross-Green's functions for the loaded tyre in Fig. 7(e) and (f), they show the same qualitative behaviour as in the unloaded case, with a larger time for the perturbation to travel towards the leading edge (against the rotation) and a shorter time to travel towards the trailing edge (with the rotation) with respect to the non-rotating situation. Also a larger amplitude and longer periods are seen compared to the unloaded case.

It can be concluded that using the Green's functions of the loaded tyre in a contact force calculation leads to smaller forces than in the unloaded case, lower frequencies are present in the response and they decrease faster as the rotational velocity increases. Furthermore, for the loaded tyre the rotational velocity leads to an asymmetry between the point-responses at the leading and trailing edge, which is not found for the unloaded tyre. These results indicate that Green's functions obtained linearising around the underformed configuration do not adequately describe the effect of load and rotational velocity on the tyre dynamic response. However, as mentioned earlier, the current FE model overestimates the softening due to loading at the contact zone, which means that the effects mentioned above will probably be less pronounced if a more accurate tyre model is used. The influence of linearising around the loaded configuration on the predicted contact forces and tyre vibrations should be investigated and compared to experimental result in order to provide definitive conclusions.

## 6. Conclusions

A closed-form expression for the Green's functions of a loaded rotating tyre expressed in the Eulerian reference frame is derived. The information needed to actually compute these Green's functions are the eigenfrequencies and eigenmodes of the loaded tyre in the tyre reference frame and the mass matrix obtained from a standard FE calculation. A non-linear FE model is used to determine the large tyre deformation due to loading and the model is linearised around the deformed state. This is different from the usual definition of the Green's functions where the tyre model is linearised around the undeformed state.

The presented formulation opens the possibility to solve the contact problem directly in the Eulerian reference frame and to include local tyre softening due to non-linear effects while keeping the computational advantage of describing the tyre dynamics as a set of impulse response functions. Solving the contact problem

in the Eulerian reference frame means that only a small submatrix of the total matrix of Green's functions is needed and that a finer mesh is only needed in the potential contact zone, which dramatically reduces the size of the matrices and, therefore, the computational requirements. Additionally the contact forces and tyre response are directly obtained in the vehicle-fixed reference frame, which allows for a direct coupling to interior noise transmission and sound radiation.

It can be concluded that using the Green's functions of the loaded tyre in a contact force calculation leads to smaller forces than in the unloaded case, lower frequencies are present in the response and they decrease faster as the rotational velocity increases. Although these effects might be less pronounced if a more accurate tyre model is used, these results indicate that Green's functions obtained linearising around the underformed configuration do not adequately describe the effect of load and rotational velocity on the tyre dynamic response. Nevertheless, the accuracy of the tyre model should be enhanced and the influence of linearising around the loaded configuration on the predicted contact forces and tyre vibrations should be investigated and compared to experimental result in order to provide definitive conclusions.

## References


Bouhaddi, N., Fillod, R., 1992. A method for selecting master dof in dynamic substructuring using the Guyan condensation method. Computers and Structures 45, 941–946.

Brinkmeier, M., Nackenhorst, U., 2004. Finite element analysis of eigendynamics of rolling tyres. In: Proceedings of Applied Mathematics Mechanics.

Brinkmeier, M., Nackenhorst, U., 2008. An approach for large-scale gyroscopic eigenvalue problems with an application to high-frequency response of rolling tyres. Computational Mechanics 41, 503–515.

Fioole, J., 2008. Experimental Modal Analysis of an Automobile Tire. Bachelor Project, Eindhoven University of Technology.

Fraggstedt, M., 2008. Vibrations, Damping and Power Dissipation in Car Tyres. Doctoral Thesis, KTH Royal Institute of Technology.

Gong, S., 1993. A Study of in-plane Dynamics of Tires. Ph.D. Thesis, Delft University of Technology.

Guyan, R., 1965. Reduction of stiffness and mass matrices. AIAA Journal 3, 380.

Kim, B., Kim, G., Lee, T., 2007. The identification of sound generating mechanisms of tyres. Applied Acoustics 68, 114–133.

Kim, Y.J., Bolton, J., 2003. Effects of rotation on the dynamics of a circular cylindrical shell with applications to tyre vibration. Journal of Sound and Vibration 275, 605–621.

Kindt, P., 2008. Structure-borne Tyre Road Noise Due to Road Surface Discontinuities. Doctoral Thesis, Department of Mechanical Engineering, Katholieke Universiteit Leuven.

Lopez, I., Blom, R., Roozen, N., Nijmeijer, H., 2007. Modelling vibrations on deformed rolling tyres – a modal approach. Journal of Sound and Vibration 307 (3–5), 481–494.

Lopez, I., van Doorn, R., van der Steen, R., Roozen, N., Nijmeijer, H., 2009. Frequency loci veering due to deformation in rotating tyres. Journal of Sound and Vibration 324 (3–5), 622–639.

Nackenhorst, U., 2004. The ALE-formulation of bodies in rolling contact: theoretical foundations and finite element approach. Computer Methods in Applied Mechanics and Engineering 193 (39–41), 4299–4322.

O'Boy, D., Dowling, A., 2009. Tyre/road interaction noise – numerical noise prediction of a patterned tyre on a rough road surface. Journal of Sound and Vibration 323 (1–2), 270–291.

Pieters, R., 2007. Experimental Modal Analysis of an Automobile Tire Under Static Load. Bachelor Project, Eindhoven University of Technology.

Pinnington, R., 2006a. A wave model of a circular tyre. Part 1: Belt modelling. Journal of Sound and Vibration 290, 101–132.

Pinnington, R., 2006b. A wave model of a circular tyre. Part 2: Side-wall and force transmission modelling. Journal of Sound and Vibration 290, 133–168.

Rustighi, E., Elliot, S., Finnveden, S., Gulyas, K., Mocsai, T., Danti, M., 2008. Linear stochastic evaluation of tyre vibration due to tyre/road excitation. Journal of Sound and Vibration 310, 1112–1127.

Sabiniarz, P., 2011. Modelling the Vibrations on a Rolling Tyre and their Relation to Exterior and Interior Noise. Doctoral Thesis, Chalmers University of Technology.

SIMULIA, 2006. Abaqus Example Problems Manual. Simulia, 6th ed.

Wullens, F., Kropp, W., 2004. A three-dimensional contact model for tyre/road interaction in rolling conditions. Acta Acustica United with Acustica 90, 702–711.

Wullens, F., Kropp, W., 2007. Wave content of the vibration field of a rolling tyre. Acta Acustica United with Acustica 93, 48–56.